

Microquasars to AGNs: An uniform Jet variability

Ajay Sharma^a, Raj Prince^b, Debanjan Bose^c

^a*S N Bose National Centre for Basic Sciences, Block JD, Salt Lake, Varanasi, 700106, West Bengal, India*

^b*Department of Physics, Institute of Science, Banaras Hindu University, Varanasi, 221005, Uttar Pradesh, India*

^c*Department of Physics, Central University of Kashmir, Ganderbal, 191131, Kashmir, India*

Abstract

The long-term variability study over a range of black hole (BH) mass systems from the microquasars of stellar-mass black holes to the Active Galactic Nuclei (AGNs) of supermassive black holes, in γ -rays offers new insights into the physics of relativistic jets. In this work, we investigate the γ -ray variability of 11 AGNs—including 7 blazars, 2 unclassified blazar candidates (BCUs), 1 radio galaxy (RG), and 1 narrow-line Seyfert 1 galaxy (NLS1) as well as 2 microquasars. We apply a stochastic process known as the Damped Random Walk (DRW) to model the ~ 15 years of Fermi-LAT light curves. The characteristic timescales observed for AGNs are comparable to those in the accretion disc. Interestingly, the timescales observed in the jet emission of microquasars are similar to those of AGNs, suggesting uniform jet properties across the black hole masses. The observed rest-frame timescales of AGNs overlap with both thermal and non-thermal timescales associated with the jet and accretion disk, respectively, suggesting a scaled relationship between τ_{DRW}^{rest} and black hole mass (M_{BH}). While the timescales observed for microquasars deviate significantly from this relationship, nonetheless exhibit a scaled $\tau_{DRW}^{rest} - M_{BH}$ relationship using γ -rays specifically. These findings offer new insights into the origin of jets and the processes driving the emission within them. Additionally, this study hints at a new perspective that the relativistic jets' properties or their production mechanisms may be independent of the black hole mass.

Keywords: Microquasars, AGN, Jet Variability, BH Mass

1. Introduction

Since the launch of Fermi Large Area Telescope (Fermi-LAT) it has become a premier instrument for studying both galactic and extragalactic sources in the high-energy regime, particularly at energies of 100 MeV and above. Observations have shown that γ -ray emissions from Active Galactic Nuclei (AGNs) dominate the extragalactic γ -ray sky. AGNs are among the most luminous objects in the universe, powered by supermassive black holes (SMBHs) at their cores. The accretion of matter onto these SMBHs is the primary energy source driving the immense luminosity of AGNs. Based on their observational properties—such as bolometric luminosity, flux variability, and broadband spectral energy distribution (SED)—AGNs are categorized into various classes.

A particularly extreme class of AGNs, known as blazars, exhibits strong Doppler-boosted non-thermal emission and rapid, high-amplitude variability across the entire electromagnetic spectrum, with timescales ranging from minutes to years. Blazars are unique in that their relativistic jets are closely aligned with the observer's line of sight (within approximately 5°) Antonucci (1993); Urry and Padovani (1995). Blazars are further subdivided into two categories: BL Lac objects (BL Lacs) and Flat Spectrum Radio Quasars (FSRQs), distinguished primarily by the strength of their optical emission lines Fossati et al. (1998); Ghisellini et al. (2017); Ajello et al. (2020).

AGN variability has been detected across the entire electromagnetic spectrum, including in jetted AGNs with relatively large inclination angles—referred to as misaligned AGNs or ra-

dio galaxies. These objects also exhibit strong and persistent flux variability in γ -rays Collaboration et al. (2018). Numerous studies have been conducted to explore the underlying physical processes that characterize the variability in these sources Abdalla et al. (2017); Yan et al. (2018); Rieger (2019); Bhatta and Dhital (2020). For instance, the Narrow-Line Seyfert 1 (NLS1) galaxy PMN J0948+0022 has been observed in gamma rays at energies above 100 MeV Foschini et al. (2012). This source has also been extensively investigated using multiwavelength observations D'Ammando et al. (2014). Lower-mass black hole systems, such as microquasars and X-ray binaries, have also been studied through multiwavelength observations Acciari et al. (2009).

γ -ray variability studies have become a crucial tool for understanding the physical processes within relativistic jets from AGNs and even microquasars. Flux variability is observed across a wide range of timescales. One effective method for quantifying this variability is through the power spectral density (PSD), which measures the amplitude of variations in a time series as a function of frequency or timescale. The PSD is particularly useful for characterizing the complex nature of emissions, which may be driven by an underlying stochastic process. In some cases, emissions exhibit an oscillatory pattern known as quasi-periodic oscillations (QPOs), which have been detected in Fermi-LAT data Ackermann et al. (2015); Sandrinelli et al. (2016); Zhou et al. (2018); Peñil et al. (2020); Banerjee et al. (2023); Prince et al. (2023). However, the reliability of these QPOs remains questionable, and the exact mechanisms behind

their production are still not well understood.

Another approach involves to understand AGN variability by modeling it with stochastic process, which has been extensively used to describe the optical variability of AGNs Kelly et al. (2009); MacLeod et al. (2010); Zu et al. (2013); Rakshit and Stalin (2017); Li and Wang (2018); Zhang et al. (2018); Lu et al. (2019); Burke et al. (2021); Zhang et al. (2023b). This method has proven particularly useful for characterizing variability across multiple wavelengths in AGN emissions. The stochastic process is typically represented by the Damped Random Walk (DRW) model, also known as the Ornstein-Uhlenbeck (OU) process, which is characterized by a break-like feature in its PSD. Generally, the PSDs of jets and accretion discs are described by a bending power law (BPL). At frequencies above the break frequency (which corresponds to a characteristic timescale), the PSD follows a power law with a slope of ~ 2 . Below the break frequency, the PSD is represented by white noise. This stochastic model effectively captures the long-term variability of AGN accretion discs.

In recent years, the DRW model has been widely applied not only in the optical time domain but also to submillimeter Chen et al. (2023), X-ray Zhang et al. (2024a), and γ -ray Sobolewska et al. (2014); Goyal et al. (2018); Ryan et al. (2019); Tarnopolski et al. (2020); Covino et al. (2020); Yang et al. (2021); Zhang et al. (2022); Sharma et al. (2024) variability in AGNs and even microquasars. These findings suggest that non-thermal timescales from jets are somehow connected to the thermal timescales of accretion discs.

The Fermi-LAT observatory has been successfully operating and observing the entire sky for over 15 yrs, offering an exceptional opportunity to study long-term gamma-ray variability in AGNs and microquasars. In this work, we apply the `celerite`¹ model Foreman-Mackey et al. (2017) to the nearly 15-yr Fermi-LAT light curves of 13 sources, including 7 blazars, 2 blazar candidates of uncertain type (BCUs), 1 radio galaxy, 1 Narrow-Line Seyfert 1 (NLS1) galaxy, and 2 microquasars. Our goal is to investigate the gamma-ray variability of these sources, explore the underlying emission processes, and establish connections between observational data and theoretical models.

The structure of this paper is as follows: Section 2 provides a brief overview of the Fermi-LAT data processing methods. Section 3 introduces the DRW model. In Section 4, we summarize the DRW modeling results for all sources in our sample. In Section 5, we discuss the observed results in detail.

2. Sample and Fermi-LAT Data Analysis

The sample in this investigation consists of 13 sources, including 12 Active Galactic Nuclei (AGNs). Among these AGNs, there are 7 Blazars, 1 Radio galaxy, 1 Narrow-line Seyfert 1 galaxies, and 2 Unclassified blazar candidates. Each of these sources demonstrates significant variability in γ -ray emissions, with detailed information available in Table Appendix A.

The Fermi-LAT observations Abdo et al. (2010) for all sources in the sample were collected over a span of ~ 15 yr (from MJD 54675 to 60460), within the energy range of 0.1-300 GeV. The analysis of the gamma-ray data was conducted using *Fermi* Science Tools, `FERMITOOLS` package². Events from the `SOURCE` class (`evclass=128`, `evtype=3`) were selected within a region of interest (ROI) of 15° for each source using the `gtselect` tool. To avoid contamination from the Earth's limb, a maximum zenith angle of 90° was applied. To ensure data quality and good time intervals (GTIs), the standard criteria with the recommended filter expression (`DATA_QUAL > 0`) && (`LAT_CONFIG == 1`) were used. The instrument response function "`P8R3_SOURCE_V3`" was utilized during data processing. The galactic diffuse emission model `gll_iem_v07.fits`³ and extra-galactic diffuse emission model `iso_P8R3_SOURCE_V3.v1.txt`³ were employed. In the likelihood analysis, the unbinned likelihood approach⁴ was performed using the `GTLIKE` tool Cash 1979; Mattox et al. 1996, which provided the significance of each source within the ROI, including the source of interest, in the form of the Test Statistic (TS), which is defined as $TS = -2\ln\left(\frac{L_{max,0}}{L_{max,1}}\right)$, where $L_{max,0}$ and $L_{max,1}$ are the maximum likelihood value for a model without an additional source and the maximum likelihood value for a model with the additional source at a specified location, respectively.

The light curves for sources are generated with a TS greater than 9 using the unbinned likelihood approach, ensuring reliable outcomes with a high signal-to-noise ratio. During the light curve generation, parameters for sources located more than 15° from the center of the Region of Interest (ROI) were fixed, while those within 10° were allowed to vary freely. The `FERMIPY`⁵ software package was utilized for this analysis.

3. Stochastic Process

The general consensus is that the variability observed in AGNs is inherently stochastic. The variability in AGNs can be explored through Continuous Time Autoregressive Moving Average [CARMA(p, q)] processes (Kelly et al., 2014), which are defined as the solutions to the following stochastic differential equation:

$$\begin{aligned} \frac{d^p y(t)}{dt^p} + \alpha_{p-1} \frac{d^{p-1} y(t)}{dt^{p-1}} + \dots + \alpha_0 y(t) = \\ \beta_q \frac{d^q \epsilon(t)}{dt^q} + \beta_{q-1} \frac{d^{q-1} \epsilon(t)}{dt^{q-1}} + \dots + \beta_0 \epsilon(t), \end{aligned} \quad (1)$$

where, the time series is given as $y(t)$, $\epsilon(t)$ represents a continuous time white-noise process, α^* and β^* are the coefficients

²<https://fermi.gsfc.nasa.gov/ssc/data/analysis/documentation/>

³<https://fermi.gsfc.nasa.gov/ssc/data/access/lat/BackgroundModels.html>

⁴https://fermi.gsfc.nasa.gov/ssc/data/analysis/scitools/likelihood_tutorial.html

⁵<https://fermipy.readthedocs.io/en/latest/>

¹<https://celerite.readthedocs.io/en/stable/>

of AR and MA models, respectively. Parameters p and q are the order of AR and MA models, respectively.

When the model's parameters are set to $p=1$ and $q=0$, it corresponds to a Continuous Auto-Regressive model CAR(1), also known as the Ornstein–Uhlenbeck process. In astronomical literature, this CAR(1) model is frequently referred to as a DRW (Damped Random Walk) process and is governed by the following stochastic differential equation (Kelly et al., 2009; Ruan et al., 2012; Moreno et al., 2019; Burke et al., 2021; Zhang et al., 2022, 2023b; Sharma et al., 2024; Zhang et al., 2024a).

$$\left[\frac{d}{dt} + \frac{1}{\tau_{DRW}} \right] y(t) = \sigma_{DRW} \epsilon(t) \quad (2)$$

where τ_{DRW} is the characteristic damping time-scale of the DRW process and σ_{DRW} is representing the amplitude of random perturbations. The covariance function of the DRW model is defined as

$$k(t_{nm}) = a \cdot \exp(-t_{nm}c), \quad (3)$$

where $t_{nm} = |t_n - t_m|$ represents the time lag between measurements m and n , with $a = 2\sigma_{DRW}^2$ and $c = \frac{1}{\tau_{DRW}}$. The power spectral density (PSD) is expressed as:

$$S(\omega) = \sqrt{\frac{2}{\pi}} \frac{a}{c} \frac{1}{1 + (\frac{\omega}{c})^2} \quad (4)$$

The PSD of DRW is a Broken Power Law (BPL) form, where the broken frequency f_b corresponds to the characteristic damping timescale $\tau_{DRW} = \frac{1}{2\pi f_b}$.

To estimate the best-fit parameters and their associated uncertainties of the DRW model for each source in our sample, we used the Markov chain Monte Carlo (MCMC) algorithm provided by the `emcee`⁶ package Foreman-Mackey et al. (2013). For the `celerite` modeling, we executed MCMC with 32 parallel chains, each running 10,000 steps for burn-in and 20,000 steps for generating the parameter distributions. In the `emcee` modeling, we determined the Maximum a posteriori (MAP) parameters using the nonlinear optimizer L-BFGS-B⁷, implemented by the `scipy` project.

4. RESULTS

We employed DRW modeling to explore the variability characteristics timescale in the γ -ray lightcurves of 7 blazars, as listed in Table Appendix A. The results are illustrated in Figure 1. To assess the quality of the DRW modeling, we analyzed the probability densities of the Autocorrelation Functions (ACF) of both the residuals and the squared residuals for all blazars. The lagged values in ACFs consistently fell within the 95% confidence interval expected for white noise. Additionally, the residuals' distribution was fitted to a normal distribution, with the resulting parameters detailed in Table Appendix

A. The distribution showed good agreement with a normal distribution, characterized by a mean (μ) value close to zero and a standard deviation (σ) less than one. This finding is further validated by the Kolmogorov–Smirnov (KS) test⁸, which was applied to evaluate the normality of the residuals. The p-values of the test observed for all blazars are greater than 0.05, indicating that the null hypothesis of normality can not be rejected, see the Table Appendix A.

A similar approach was applied to analyze the light curves of non-blazars and microquasars, and the results are presented in Figure 2 and Table Appendix A. For a few sources, the observed lagged values in the ACFs fall outside the 95% confidence interval, suggest that the model may not have adequately captured the flaring episodes in the light curve, or indicate that the events observed in the light curve are stochastic in nature.

The posterior probability density distributions of the parameters obtained from the modeling using the MCMC algorithm are displayed in the Figure 4 and the best-fitting values are listed in Table Appendix A.

Figure 1, 2 present these findings in three columns with two rows for each source. The leftmost column displays the γ -ray lightcurve fitted with the DRW model in the top row, with the corresponding residuals shown in the bottom row. The middle column shows the distribution of the residuals alongside the best-fit normal distribution profile. The rightmost column features the ACFs of the residuals and the squared residuals.

However, it's important to consider how the limited length of a light curve can influence the modeling results. Insufficient length can bias the measurement of the damping timescale, leading to potential inaccuracies Kozłowski (2017); Suberlak et al. (2021). To ensure the reliability of the characteristic timescale measurement, we followed the criteria established by Burke et al. (2021). According to this criteria, the length of the light curve should be at least 10 times the timescale of interest ($\tau_{DRW} < 0.1 \times \text{baseline}$) and the observed damping timescale should be greater than the average cadence of the light curve ($\tau_{DRW} > \text{cadence}$). The mean cadence and baseline of each source in our sample is given in the Table Appendix A. We identified biased regions corresponding to timescales greater than 20% of the light curve length and less than the mean cadence. As shown in Figure 4, the shaded areas in the Power Spectral Density (PSD) indicate unreliable regions where the PSD is not adequately sampled. For all sources in our sample, the observed damping timescale values fall outside these unreliable regions, suggesting that the model effectively captured the characteristics of the light curve.

Applying the reliability criteria in the estimation of variability timescale as mentioned above, we obtained the damping timescale for 7 Blazars, 2 BCUs, 1 Radio galaxy, 1 Narrow-line 1 galaxy, and 2 Microquasars. The observed damping timescale (τ_{DRW}) of our sources in observer's frame of reference spans from 40 to ~ 300 days, which is reliable according to Burke et al. (2021). However, since the characteristic timescale of variability was obtained in the observer's frame, it must be corrected

⁶<https://emcee.readthedocs.io/en/stable/>

⁷<https://docs.scipy.org/doc/scipy/reference/optimize.minimize-lbfgsb.html>

⁸<https://docs.scipy.org/doc/scipy/reference/generated/scipy.stats.kstest.html>

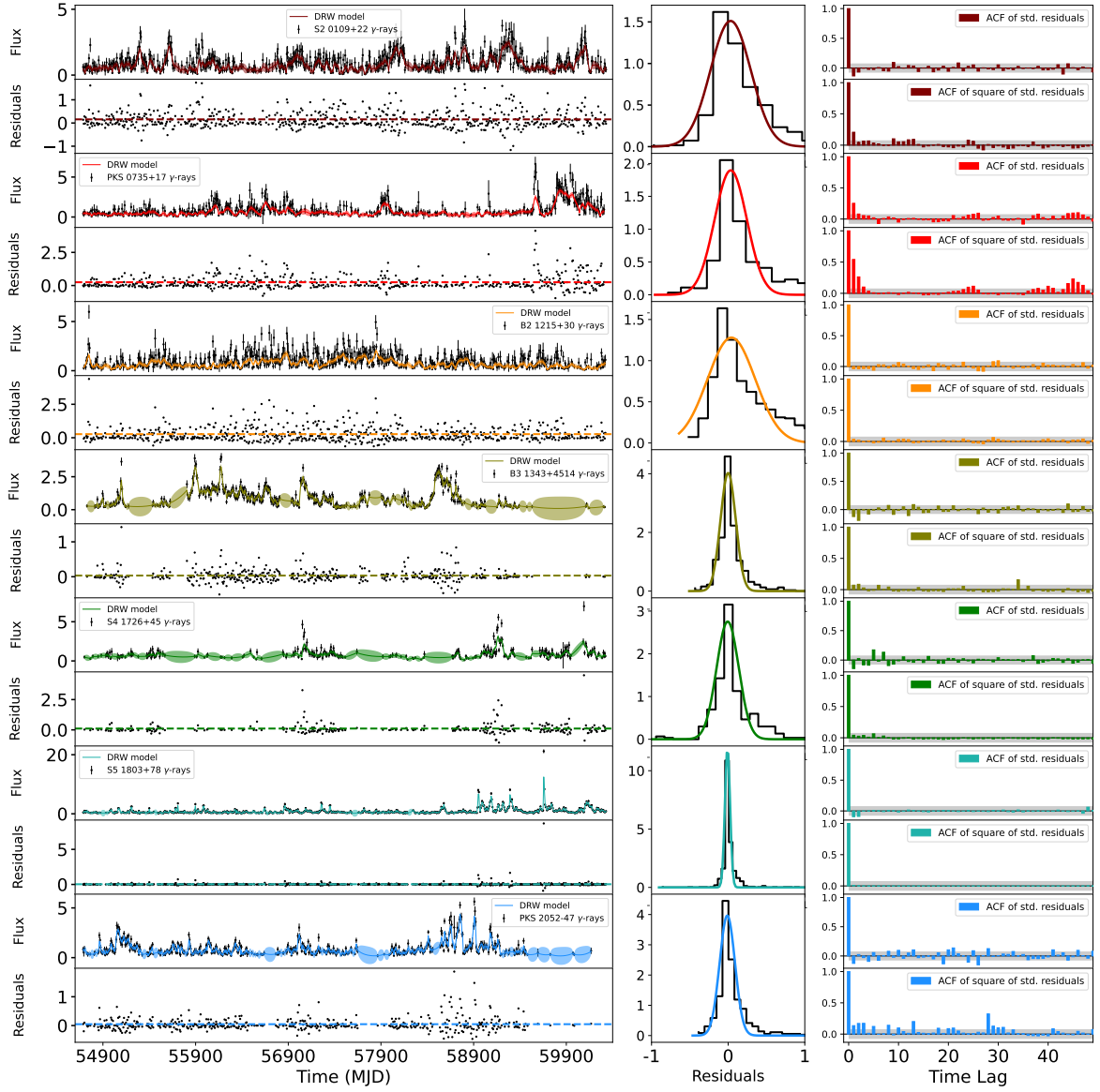


Figure 1: Results of the DRW model fitting for all blazars in our sample, Table Appendix A. Each source results are depicted in three columns: the leftmost column shows the observed γ -ray flux (black points) and the DRW-modeled light curve (in assigned colors). The bottom panel presents the residuals (black dots) with their mean in the corresponding color. The middle column displays the residuals' distribution (black histogram) alongside the best-fit normal distribution (in corresponding color). The rightmost column features the autocorrelation functions (ACFs) of the residuals and squared residuals (in assigned colors) with the 95% confidence interval for white noise (in grey). The results from modeling all blazars with the DRW model are displayed in distinct colors for enhanced visual clarity.

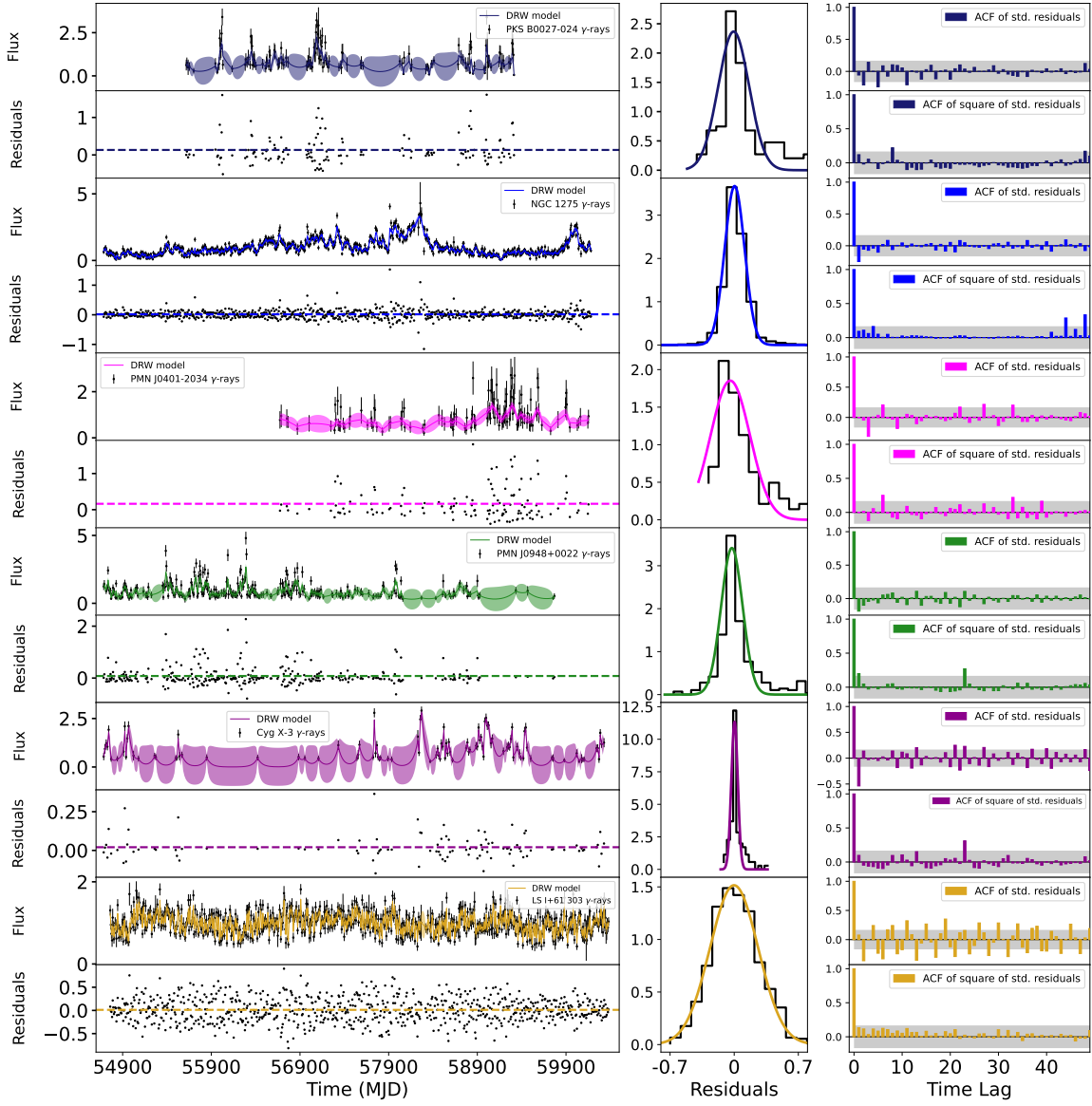


Figure 2: Results of DRW model fitting for all non-blazar sources in our sample are shown in Table Appendix A. The results are displayed in different colors as those in Figure 1.

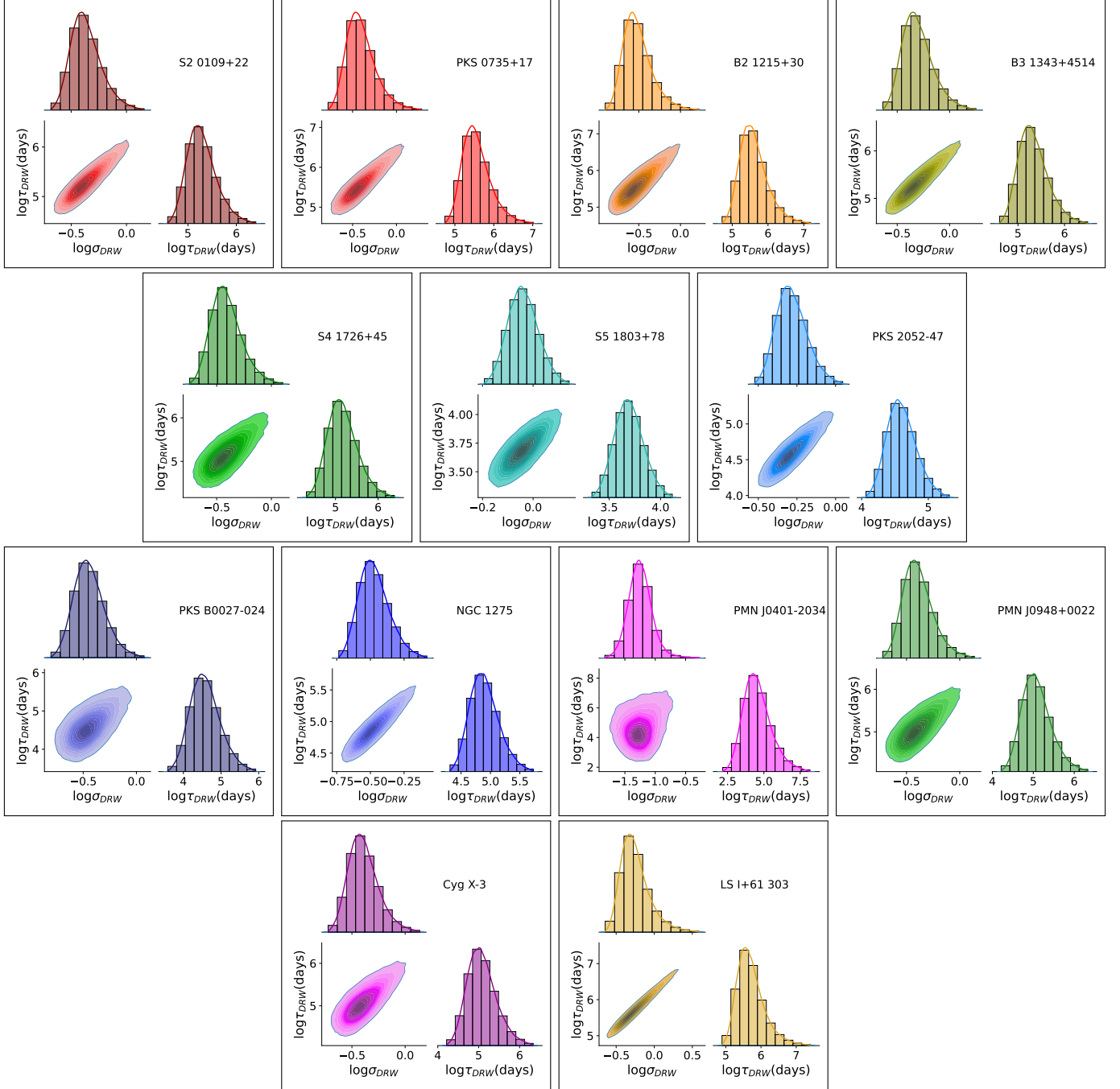


Figure 3: Posterior probability densities of the DRW model parameters for all sources in our sample, represented with the corresponding colors.

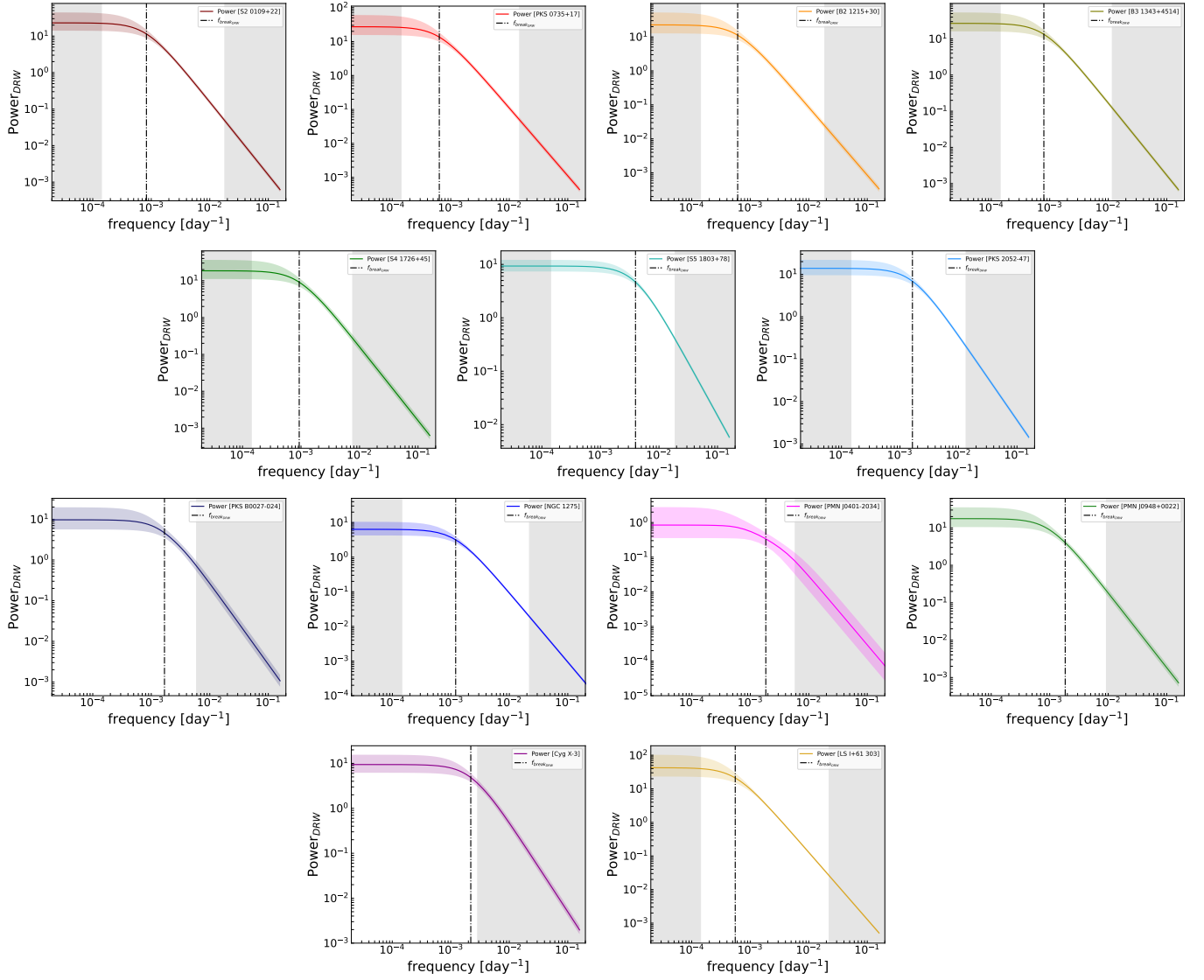


Figure 4: The PSDs of γ -rays, derived from the DRW modeling results, are presented in this figure. Each PSD profile is shown with a shaded region representing the 1σ confidence interval, corresponding to the respective colors. Additionally, two grey-shaded regions in each panel indicate the biased regions caused by the limited length and mean cadence of the light curve. A dotted vertical line marks the break frequency in the PSD.

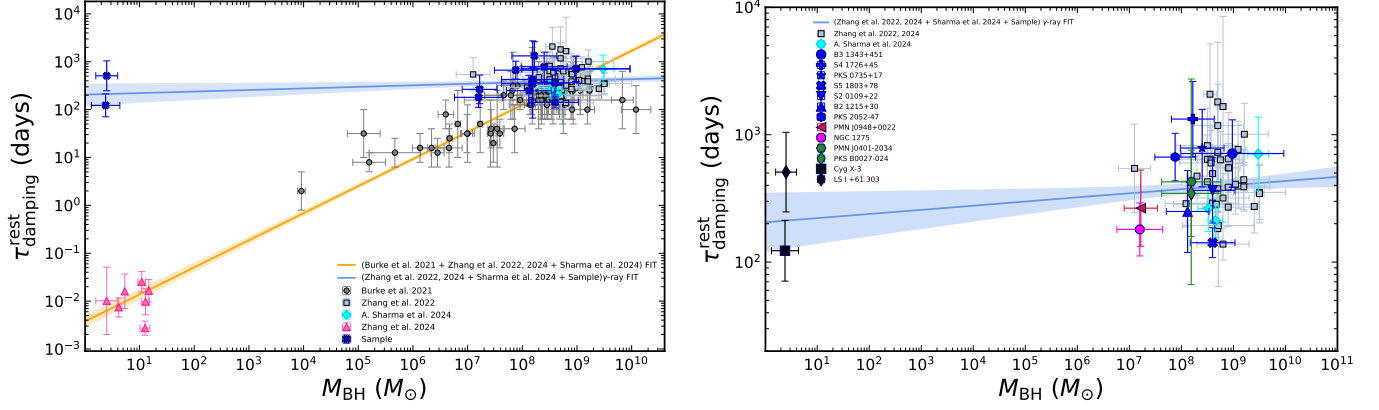


Figure 5: The figure shows the observed τ_{DRW}^{rest} as a function of M_{BH} . Data points from different studies are distinguished by various colors and shapes: grey, light blue, cyan, and light pink correspond to Burke et al. (2021); Zhang et al. (2022); Sharma et al. (2024); Zhang et al. (2024a), respectively. In the left panel, an orange line represents a combined fit to the findings from these studies, while the blue line with 1σ confidence interval, shows the fit based solely on the γ -ray results from our sample and Zhang et al. (2022); Sharma et al. (2024). The right panel illustrates the same combined fit to the γ -ray data exclusively, with sources from different classes in our sample indicated by distinct colors and shapes: blazars (blue), NLS1 galaxy (red), radio galaxy (magenta), BCUs (green), and microquasars (black).

for the Doppler beaming effect and redshift of each source to determine the timescale in the rest frame. This can be calculated using the following equation:

$$\tau_{damping}^{rest} = \frac{\tau_{obs}}{1+z} \delta_D \quad (5)$$

where z is the redshift of the source and δ_D is the Doppler factor. Estimating the Doppler factor for AGNs is a challenging task, often involving various methods such as modeling the broadband SED Chen (2018); Pei et al. (2020); Zhang et al. (2020) and constraining the equipartition brightness temperature of radio flares Lioudakis et al. (2017a). Despite these approaches, determining the Doppler factor remains subject to significant uncertainties. For the sources in our sample, we used the δ_D values obtained from a literature survey, with references provided in Table Appendix A. The variability timescale in optical observations from AGN accretion disc has been extensively studied Collier and Peterson (2001); Kelly et al. (2009); MacLeod et al. (2010); Simm et al. (2016); Suberlak et al. (2021); Burke et al. (2021); Zhang et al. (2023b). More recently, similar studies have been conducted in the submillimeter range Chen et al. (2023), X-rays Zhang et al. (2024a), and γ -rays Ryan et al. (2019); Zhang et al. (2022); Sharma et al. (2024); Zhang et al. (2024a). In this study, we analyzed the γ -ray light curves of 11 AGNs and 2 microquasars and observed timescale value for microquasars is similar to AGN. When comparing our observed γ -ray rest-frame timescales, calculated using Equation (1), with the findings from Burke et al. (2021), Zhang et al. (2022), Sharma et al. (2024), and Zhang et al. (2024a), the fit was not very satisfactory. This discrepancy is due to significant variations in the damping timescales across different wavebands for microquasars. Consequently, we fit our variability timescale data exclusively with γ -ray variability timescales. The best-fit curve, shown as a blue line with a 1σ confidence interval, the right panel in Figure 5. The best-fitting relation is

$$\tau_{damping}^{rest} = 346.54_{-48.11}^{+41.91} \left(\frac{M}{10^8 M_{\odot}} \right)^{0.06_{-0.03}^{+0.03}} \quad (6)$$

with an intrinsic scatter of 0.17 ± 0.041 and a Pearson correlation coefficient $r=0.206$, indicating a weak or no correlation between variability timescale in γ -rays and Black Hole mass, as shown in Figure 5. In our investigation, the observed τ_{DRW} values for NGC 1275 and B2 1215+30 are differ from the findings in the literature Zhang et al. (2022) and Zhang et al. (2024a), respectively. This discrepancy may be due to the use of longer light curves.

5. DISCUSSION

This work is a follow-up to our previous study Sharma et al. (2024), where we modeled the γ -ray light curves of three blazars with the DRW model and compared the results with findings from the literature. That study inspired us to further investigate the variability characteristics of different classes of AGNs and expand it to include the stellar black hole mass systems. To achieve this, we utilized over a decade of γ -ray light curve data from the Fermi-LAT observatory. While Fermi-LAT detections are predominantly blazars, it has also successfully captured several non-blazar sources. By analyzing these diverse sources, we aim to understand the emission processes responsible for the observed variations in their light curves.

In this work, We present a comprehensive investigation focused on characterizing the γ -ray variability of 7 blazars, 1 radio galaxy, 1 narrow-line Seyfert 1 galaxy, and 2 unclassified blazar candidates, and 2 microquasars. Such studies offer valuable insights into the high-energy emission regions within relativistic jets and the inner jet structure. It is widely believed that black holes, from stellar mass to supermassive, are often associated with relativistic jets. This study provides indirect evidence supporting a universal scaling law, suggesting that the jet production mechanism is invariant of their black hole mass.

The Gaussian Process (GP) method has been extensively used to characterize variability across different wavebands in a wide range of astrophysical objects, from low-mass microquasars to AGNs with supermassive black holes. It serves as a powerful tool for studying the statistical properties of variability in these objects. Several studies have been carried out to explore the characteristic timescale of optical variability Collier and Peterson (2001); Kelly et al. (2009); MacLeod et al. (2010); Simm et al. (2016); Goyal et al. (2018); Ryan et al. (2019); Covino et al. (2020); Tarnopolski et al. (2020); Suberlak et al. (2021); Burke et al. (2021); Yang et al. (2021); Zhang et al. (2023b). Ruan et al. (2012) modeled optical light curves from December 2002 to March 2008 and observed variability timescales longer than those found in Fermi-detected blazars. Xiong et al. (2015) identified significant differences in physical properties such as redshift, black hole mass, jet kinetic power, and broad-line luminosity between Fermi-detected and non-Fermi-detected blazars. Paliya et al. (2017) reported that non-Fermi-detected blazars tend to have smaller Doppler factors. Burke et al. (2021) suggested that the DRW damping timescale, measured from accretion disc variability in normal quasars, may correspond to the thermal instability timescale predicted by AGN standard accretion disc theory.

Chen et al. (2023) explored accretion physics by investigating submillimeter variability in low-luminosity AGNs, finding that the submillimeter emission has a significantly shorter variability timescale compared to optical emission, likely linked to the innermost regions of the black hole system. They also examined X-ray variability and found it to exhibit similarly short timescales, indicating that similar processes may be driving both emissions.

Further, Zhang et al. (2024a) extended similar kind of study to microquasars with X-rays, observing a scaling relationship, $\tau \propto M_{BH}$, consistent with Burke et al. (2021), suggesting that the accretion disc's variability may imprint on jet emission or be associated with physical processes occurring within the jet.

Ryan et al. (2019) analyzed Fermi-LAT observations of 13 blazars over ~ 9.5 years, Zhang et al. (2022) examined a sample of 23 AGNs, including 22 blazars and 1 radio galaxy, with Fermi-LAT data spanning approximately ~ 12.7 years, and Sharma et al. (2024) used ~ 15 -year-long γ -ray light curves of 3 blazars, all modeled using stochastic processes. These samples cover a black hole mass range from $\sim 10^7$ to $10^{10} M_{\odot}$. The variability timescales obtained from these models align with the thermal timescales on the $\tau_{DRW}^{rest} - M_{BH}$ plane, as described by Burke et al. (2021), suggesting a strong association with accretion disk variations. This connection can be explained by propagating fluctuation models Lyubarskii (1997), where the jet launching site is in close proximity to the accretion disk, leading to the imprinting of accretion disk variations on jet emissions Kataoka et al. (2001). Several accretion disk models, such as those proposed by Shakura and Sunyaev (1973); Siemiginowska et al. (1996); Kataoka et al. (2001); Hirose et al. (2009), are likely candidates for explaining such variability features. If the variability originates in the relativistic jet, the observed timescale would be influenced by the jet's Doppler factor, which is often uncertain Liodakis and Pavlidou (2015).

Variations in jet emission could be driven by fluctuations in magnetic field strength, electron injection rate, or Doppler factor Mastichiadis and Kirk (1997).

The derived damping timescales from the γ -ray emissions of all sources in our sample are plotted against M_{BH} in Figure 5. In this figure, the timescales for high-mass AGNs overlap with the thermal timescales from Burke et al. (2021) and the non-thermal timescales from Zhang et al. (2022) and Sharma et al. (2024). Additionally, the X-ray variability timescales from microquasars, as reported by Zhang et al. (2024a), are also included in the $\tau_{DRW}^{rest} - M_{BH}$ plot. These X-ray timescales exhibit a relationship with both thermal and non-thermal timescales from earlier studies and our own findings in high-mass AGNs. As discussed in Section 4, the observed γ -ray variability timescales in both microquasars are comparable in magnitude to those in high-mass AGNs and are significantly larger than the timescales observed in other wavebands.

We first compared the characteristic time scale among various types of AGN and it was found that the luminous FSRQ, NLSy1, radio galaxy, and unknown blazar type also show a similar variability time scale, referring to the fact that jet properties remain the same across the AGN types. The jet luminosity among these objects can differ however, the variability pattern remains universal.

We also included stellar mass black holes and estimated their timescales in the γ -ray emission of microquasars Cyg X-3 and LS I+61 303 that were not detected earlier. The rest-frame timescales for both the objected are approximately 186 days and 446 days, respectively. These timescales are comparable to those observed in AGNs. Figure 5 shows a best-fitting correlation between the γ -ray timescales of low-mass microquasars and high-mass AGNs. This raises the question of whether the emission from relativistic jets depends on the mass of the host black hole. Are the emission mechanisms within the jets or the processes involved in jet production independent of black hole mass? These are critical questions that need to be addressed.

Liodakis et al. (2017b) found a strong correlation between the intrinsic broadband radio luminosity of blazars and black hole mass, extending this relationship to the stellar black hole mass systems like microquasars. This finding imposes significant constraints on alternative jet models. This study suggests that the jet production mechanism is a universal process common in all black hole systems independent to their black hole mass and AGNs also operate in a similar accretion regime as the hard state in microquasars. This proposed methodology also stand out as an independent method for estimating the Doppler factor.

The findings from this investigation also suggest indirect evidence that the variability observed in γ -rays, driven by physical processes within relativistic jets, may be universal across black hole systems, regardless of their mass. While jets in microquasars extend over shorter distances compared to those in AGNs, they are still efficient enough to produce similar emission variations. It is also possible that the observed variability in both microquasars and AGNs arise from distinct processes occurring in different emission regions or within the jets themselves.

6. CONCLUSION

We present the γ -ray variability of 11 AGNs (FSRQ, BCUs, NLSy1, and radio galaxy) and 2 microquasars utilizing ~ 15 yr of the Fermi-LAT light curve. To characterize this variability, we modeled the light curves with a DRW model. Our main findings are pointed out below.

- We noted that even though FSRQs, BCUs, NLSy1, and radio galaxies are of different kinds. but the jets they host have similar properties.
- Our findings indicate that the observed characteristic variability timescales for both AGNs and microquasars are remarkably similar, irrespective of their black hole masses.
- This suggests that common underlying processes may be responsible for the observed variations in γ -ray emissions across these sources.
- The same variability time scale in stellar Black hole and supermassive black hole suggests the jet possibly can be produced by a similar procedure.

Acknowledgements

We acknowledge the various software used for the analysis and the Fermi-LAT archival data center.

References

- Abdalla, H., Abramowski, A., Aharonian, F., Benkhali, F.A., Akhperjanian, A., Andersson, T., Angüner, E., Arrieta, M., Aubert, P., Backes, M., et al., 2017. Characterizing the γ -ray long-term variability of pks 2155- 304 with hess and fermi-lat. *Astronomy & Astrophysics* 598, A39.
- Abdo, A., Ackermann, M., Agudo, I., Ajello, M., Aller, H., Aller, M., Angelakis, E., Arkharov, A., Axelsson, M., Bach, U., et al., 2010. The spectral energy distribution of fermi bright blazars. *The Astrophysical Journal* 716, 30.
- Acciari, V., Aliu, E., Arlen, T., Bautista, M., Beilicke, M., Benbow, W., Böttcher, M., Bradbury, S., Bugaev, V., Butt, Y., et al., 2009. Multiwavelength observations of ls i+ 61 303 with veritas, swift, and rxte. *The Astrophysical Journal* 700, 1034.
- Ackermann, M., Ajello, M., Albert, A., Atwood, W., Baldini, L., Ballet, J., Barbiellini, G., Bastieri, D., Gonzalez, J.B., Bellazzini, R., et al., 2015. Multiwavelength evidence for quasi-periodic modulation in the gamma-ray blazar pg 1553+ 113. *The Astrophysical Journal Letters* 813, L41.
- Ajello, M., Angioni, R., Axelsson, M., Ballet, J., Barbiellini, G., Bastieri, D., Gonzalez, J.B., Bellazzini, R., Bissaldi, E., Bloom, E., et al., 2020. The fourth catalog of active galactic nuclei detected by the fermi large area telescope. *The Astrophysical Journal* 892, 105.
- Antonucci, R., 1993. Unified models for active galactic nuclei and quasars. In: *Annual review of astronomy and astrophysics*. Vol. 31 (A94-12726 02-90), p. 473-521. 31, 473-521.
- Banerjee, A., Sharma, A., Mandal, A., Das, A.K., Bhatta, G., Bose, D., 2023. Detection of periodicity in the gamma-ray light curve of the bl lac 4fgl j2202.7+ 4216. *Monthly Notices of the Royal Astronomical Society: Letters* 523, L52-L57.
- Bhatta, G., Dhital, N., 2020. The nature of γ -ray variability in blazars. *The Astrophysical Journal* 891, 120.
- Burke, C.J., Shen, Y., Blaes, O., Gammie, C.F., Horne, K., Jiang, Y.F., Liu, X., McHardy, I.M., Morgan, C.W., Scaringi, S., et al., 2021. A characteristic optical variability time scale in astrophysical accretion disks. *Science* 373, 789-792.
- Cash, W., 1979. Parameter estimation in astronomy through application of the likelihood ratio. *Astrophysical Journal, Part 1*, vol. 228, Mar. 15, 1979, p. 939-947. 228, 939-947.
- Chai, B., Cao, X., Gu, M., 2012. What governs the bulk velocity of the jet components in active galactic nuclei? *The Astrophysical Journal* 759, 114.
- Chen, B.Y., Bower, G.C., Dexter, J., Markoff, S., Ridenour, A., Gurwell, M.A., Rao, R., Wallström, S.H., 2023. Testing the linear relationship between black hole mass and variability timescale in low-luminosity agns at submillimeter wavelengths. *The Astrophysical Journal* 951, 93.
- Chen, L., 2018. On the jet properties of γ -ray-loud active galactic nuclei. *The Astrophysical Journal Supplement Series* 235, 39.
- Collaboration, M., Ansoldi, S., Antonelli, L., Arcaro, C., Baack, D., Babić, A., Banerjee, B., Bangale, P., Barres de Almeida, U., Barrio, J., et al., 2018. The broad-band properties of the intermediate synchrotron peaked bl lac s2 0109+ 22 from radio to vhe gamma-rays. *Monthly Notices of the Royal Astronomical Society* 480, 879-892.
- Collier, S., Peterson, B.M., 2001. Characteristic ultraviolet/optical timescales in active galactic nuclei. *The Astrophysical Journal* 555, 775.
- Costamante, L., Cutini, S., Tosti, G., Antolini, E., Tramacere, A., 2018. On the origin of gamma-rays in fermi blazars: beyond the broad-line region. *Monthly Notices of the Royal Astronomical Society* 477, 4749-4767.
- Covino, S., Landoni, M., Sandrinelli, A., Treves, A., 2020. Looking at blazar light-curve periodicities with gaussian processes. *The Astrophysical Journal* 895, 122.
- D'Ammando, F., Larsson, J., Orienti, M., Raiteri, C., Angelakis, E., Carramiana, A., Carrasco, L., Drake, A., Fuhrmann, L., Giroletti, M., et al., 2014. Multiwavelength observations of the γ -ray-emitting narrow-line seyfert 1 pnn j0948+ 0022 in 2011. *Monthly Notices of the Royal Astronomical Society* 438, 3521-3534.
- Doi, A., Nakahara, S., Nakamura, M., Kino, M., Kawakatu, N., Nagai, H., 2019. Radio jet structures at 100 pc and larger scales of the γ -ray-emitting narrow-line seyfert 1 galaxy pnn j0948+ 0022. *Monthly Notices of the Royal Astronomical Society* 487, 640-649.
- Fan, J.H., Yang, J.H., Liu, Y., Zhang, J.Y., 2013. The gamma-ray doppler factor determinations for a fermi blazar sample. *Research in Astronomy and Astrophysics* 13, 259.
- Foreman-Mackey, D., Agol, E., Ambikasaran, S., Angus, R., 2017. Fast and scalable gaussian process modeling with applications to astronomical time series. *The Astronomical Journal* 154, 220.
- Foreman-Mackey, D., Hogg, D.W., Lang, D., Goodman, J., 2013. emcee: the mcmc hammer. *Publications of the Astronomical Society of the Pacific* 125, 306.
- Foschini, L., Angelakis, E., Fuhrmann, L., Ghisellini, G., Hovatta, T., Lahteenmaki, A., Lister, M., Braitto, V., Gallo, L., Hamilton, T., et al., 2012. Radio-to- γ -ray monitoring of the narrow-line seyfert 1 galaxy pnn j0948+ 0022 from 2008 to 2011. *Astronomy & Astrophysics* 548, A106.
- Fossati, G., Maraschi, L., Celotti, A., Comastri, A., Ghisellini, G., 1998. A unifying view of the spectral energy distributions of blazars. *Monthly Notices of the Royal Astronomical Society* 299, 433-448.
- Furniss, A., Worsack, G., Fumagalli, M., Johnson, C., Williams, D., Pontrelli, P., Prochaska, J., 2019. Spectroscopic redshift of the gamma-ray blazar b2 1215+ 30 from ly α emission. *The Astronomical Journal* 157, 41.
- Ghisellini, G., Righi, C., Costamante, L., Tavecchio, F., 2017. The fermi blazar sequence. *Monthly Notices of the Royal Astronomical Society* 469, 255-266.
- Ghisellini, G., Tavecchio, F., Foschini, L., Ghirlanda, G., Maraschi, L., Celotti, A., 2010. General physical properties of bright fermi blazars. *Monthly Notices of the Royal Astronomical Society* 402, 497-518.
- Goyal, A., Zola, S., Marchenko, V., Soida, M., Nilsson, K., Ciprini, S., Baran, A., Ostrowski, M., Wiita, P., Siemiginowska, A., et al., 2018. Stochastic modeling of multiwavelength variability of the classical bl lac object oj 287 on timescales ranging from decades to hours. *The Astrophysical Journal* 863, 175.
- Hirose, S., Krolik, J.H., Blaes, O., 2009. Radiation-dominated disks are thermally stable. *The Astrophysical Journal* 691, 16.
- Kadowaki, L.H., Dal Pino, E.d.G., Singh, C.B., 2015. The role of fast magnetic reconnection on the radio and gamma-ray emission from the nuclear regions of microquasars and low luminosity agns. *The Astrophysical Journal* 802, 113.
- Kataoka, J., Takahashi, T., Wagner, S.J., Iyomoto, N., Edwards, P.G., Hayashida, K., Inoue, S., Madejski, G.M., Takahara, F., Tanihata, C., et al.,

2001. Characteristic x-ray variability of tev blazars: Probing the link between the jet and the central engine. *The Astrophysical Journal* 560, 659.
- Kelly, B.C., Bechtold, J., Siemiginowska, A., 2009. Are the variations in quasar optical flux driven by thermal fluctuations? *The Astrophysical Journal* 698, 895.
- Kelly, B.C., Becker, A.C., Sobolewska, M., Siemiginowska, A., Uttley, P., 2014. Flexible and scalable methods for quantifying stochastic variability in the era of massive time-domain astronomical data sets. *The Astrophysical Journal* 788, 33.
- Koljonen, K.I., Tomsick, J.A., 2020. The obscured x-ray binaries v404 cyg, cyg x-3, v4641 sgr, and grs 1915+ 105. *Astronomy & Astrophysics* 639, A13.
- Kozłowski, S., 2017. Limitations on the recovery of the true agn variability parameters using damped random walk modeling. *Astronomy & Astrophysics* 597, A128.
- Li, Y.R., Wang, J.M., 2018. A new approach for measuring power spectra and reconstructing time series in active galactic nuclei. *Monthly Notices of the Royal Astronomical Society: Letters* 476, L55–L59.
- Lin, C., Fan, J.H., Xiao, H.B., 2017. The intrinsic γ -ray emissions of fermi blazars. *Research in Astronomy and Astrophysics* 17, 066.
- Liodakis, I., Marchili, N., Angelakis, E., Fuhrmann, L., Nestoras, I., Myserlis, I., Karamanavis, V., Krichbaum, T., Sievers, A., Ungerechts, H., et al., 2017a. F-gamma: variability doppler factors of blazars from multiwavelength monitoring. *Monthly Notices of the Royal Astronomical Society* 466, 4625–4632.
- Liodakis, I., Pavlidou, V., 2015. Population statistics of beamed sources—ii. evaluation of doppler factor estimates. *Monthly Notices of the Royal Astronomical Society* 454, 1767–1777.
- Liodakis, I., Pavlidou, V., Papadakis, I., Angelakis, E., Marchili, N., Zensus, J.A., Fuhrmann, L., Karamanavis, V., Myserlis, I., Nestoras, I., et al., 2017b. Scale invariant jets: from blazars to microquasars. *The Astrophysical Journal* 851, 144.
- Lu, K.X., Huang, Y.K., Zhang, Z.X., Wang, K., Du, P., Hu, C., Xiao, M., Li, Y.R., Bai, J.M., Bian, W.H., et al., 2019. Supermassive black holes with high accretion rates in active galactic nuclei. x. optical variability characteristics. *The Astrophysical Journal* 877, 23.
- Lyubarskii, Y.E., 1997. Flicker noise in accretion discs. *Monthly Notices of the Royal Astronomical Society* 292, 679–685.
- MacLeod, C.L., Ivezić, Ž., Kochanek, C., Kozłowski, S., Kelly, B., Bullock, E., Kimball, A., Sesar, B., Westman, D., Brooks, K., et al., 2010. Modeling the time variability of sdss stripe 82 quasars as a damped random walk. *The Astrophysical Journal* 721, 1014.
- Massi, M., Migliari, S., Chernyakova, M., 2017. The black hole candidate 1s i+ 61 303. *Monthly Notices of the Royal Astronomical Society* 468, 3689–3693.
- Mastichiadis, A., Kirk, J., 1997. Variability in the synchrotron self-compton model of blazar emission. *Astronomy and Astrophysics*, v. 320, p. 19–25 320, 19–25.
- Mattox, J.R., Bertsch, D., Chiang, J., Dingus, B., Digel, S., Esposito, J., Fierro, J., Hartman, R., Hunter, S., Kanbach, G., et al., 1996. The likelihood analysis of egret data. *Astrophysical Journal* v. 461, p. 396 461, 396.
- Molina, E., del Palacio, S., Bosch-Ramon, V., 2019. A model for high-mass microquasar jets under the influence of a strong stellar wind. *Astronomy & Astrophysics* 629, A129.
- Moreno, J., Vogeley, M.S., Richards, G.T., Yu, W., 2019. Stochastic modeling handbook for optical agn variability. *Publications of the Astronomical Society of the Pacific* 131, 063001.
- Paliya, V.S., Marcotulli, L., Ajello, M., Joshi, M., Sahayanathan, S., Rao, A., Hartmann, D., 2017. General physical properties of cgrabs blazars. *The Astrophysical Journal* 851, 33.
- Pei, Z., Fan, J., Yang, J., Bastieri, D., 2020. The estimation of γ -ray doppler factor for fermi/lat-detected blazars. *Publications of the Astronomical Society of Australia* 37, e043.
- Peña-Herazo, H.A., Paggi, A., García-Pérez, A., Amaya-Almazán, R.A., Mas-saro, F., Ricci, F., Chavushyan, V., Marchesini, E.J., Masetti, N., Landoni, M., et al., 2021. Optical spectroscopic observations of gamma-ray blazar candidates. xi. optical observations from soar, blanco, ntt and oan-spm. the story so far. *The Astronomical Journal* 162, 177.
- Peñil, P., Domínguez, A., Buson, S., Ajello, M., Otero-Santos, J., Barrio, J., Nemmen, R., Cutini, S., Rani, B., Frankowiak, A., et al., 2020. Systematic search for γ -ray periodicity in active galactic nuclei detected by the fermi large area telescope. *The Astrophysical Journal* 896, 134.
- Prince, R., Banerjee, A., Sharma, A., Gupta, A.C., Bose, D., et al., 2023. Quasi-periodic oscillation detected in γ -rays in blazar pks 0346- 27. *Astronomy & Astrophysics* 678, A100.
- Rakshit, S., Stalin, C., 2017. Optical variability of narrow-line and broad-line seyfert 1 galaxies. *The Astrophysical Journal* 842, 96.
- Rieger, F.M., 2019. Gamma-ray astrophysics in the time domain. *Galaxies* 7, 28.
- Ruan, J.J., Anderson, S.F., MacLeod, C.L., Becker, A.C., Burnett, T., Davenport, J.R., Ivezić, Ž., Kochanek, C.S., Plotkin, R.M., Sesar, B., et al., 2012. Characterizing the optical variability of bright blazars: Variability-based selection of fermi active galactic nuclei. *The Astrophysical Journal* 760, 51.
- Ryan, J.L., Siemiginowska, A., Sobolewska, M., Grindlay, J., 2019. Characteristic variability timescales in the gamma-ray power spectra of blazars. *The Astrophysical Journal* 885, 12.
- Sahakyan, N., Harutyunyan, G., Israelyan, D., Khachatryan, M., 2020. Exploring the origin of multiwavelength emission from high-redshift blazar b3 1343+ 451. *Astrophysics* 63, 334–348.
- Sandrinelli, A., Covino, S., Dotti, M., Treves, A., 2016. Quasi-periodicities at year-like timescales in blazars. *The Astronomical Journal* 151, 54.
- Shakura, N.I., Sunyaev, R.A., 1973. Black holes in binary systems. observational appearance. *Astronomy and Astrophysics*, Vol. 24, p. 337–355 24, 337–355.
- Sharma, A., Kamaram, S.R., Prince, R., Khatoon, R., Bose, D., 2024. Probing the disc–jet coupling in s4 0954+ 65, pks 0903- 57, and 4c+ 01.02 with γ -rays. *Monthly Notices of the Royal Astronomical Society* 527, 2672–2686.
- Siemiginowska, A., Czerny, B., Kostyunin, V., 1996. Evolution of an accretion disk in an active galactic nucleus. *Astrophysical Journal* v. 458, p. 491 458, 491.
- Simm, T., Salvato, M., Saglia, R., Ponti, G., Lanzuisi, G., Trakhtenbrot, B., Nandra, K., Bender, R., 2016. Pan-starrs1 variability of xmm-cosmos agn-ii. physical correlations and power spectrum analysis. *Astronomy & Astrophysics* 585, A129.
- Sobolewska, M.A., Siemiginowska, A., Kelly, B.C., Nalewajko, K., 2014. Stochastic modeling of the fermi/lat γ -ray blazar variability. *The Astrophysical Journal* 786, 143.
- Suberlak, K.L., Ivezić, Ž., MacLeod, C., 2021. Improving damped random walk parameters for sdss stripe 82 quasars with pan-starrs1. *The Astrophysical Journal* 907, 96.
- Tarnopolski, M., Żywuca, N., Marchenko, V., Pascual-Granado, J., 2020. A comprehensive power spectral density analysis of astronomical time series. i. the fermi-lat gamma-ray light curves of selected blazars. *The Astrophysical Journal Supplement Series* 250, 1.
- Urry, C.M., Padovani, P., 1995. Unified schemes for radio-loud active galactic nuclei. *Publications of the Astronomical Society of the Pacific* 107, 803.
- Valverde, J., Horan, D., Bernard, D., Fegan, S., Abeysekera, A., Archer, A., Benbow, W., Bird, R., Brill, A., Brose, R., et al., 2020. A decade of multiwavelength observations of the tev blazar 1es 1215+ 303: Extreme shift of the synchrotron peak frequency and long-term optical–gamma-ray flux increase. *The Astrophysical Journal* 891, 170.
- Wang, G., Cai, J., Fan, J., 2022. A possible 3 yr quasi-periodic oscillation in γ -ray emission from the fsrq s5 1044+ 71. *The Astrophysical Journal* 929, 130.
- Xiao, H., Ouyang, Z., Zhang, L., Fu, L., Zhang, S., Zeng, X., Fan, J., 2022. The relativistic jet and central engine of fermi blazars. *The Astrophysical Journal* 925, 40.
- Xin, Y.X., Xiong, D.R., Bai, J.M., Liu, H.T., Lu, K.X., Mao, J.R., 2022. Multicolor optical monitoring of the γ -ray emitting narrow-line seyfert 1 galaxy pmn j0948+ 0022 from 2020 to 2021. *Research in Astronomy and Astrophysics* 22, 075001.
- Xiong, D., Zhang, X., 2014. Intrinsic γ -ray luminosity, black hole mass, jet and accretion in fermi blazars. *Monthly Notices of the Royal Astronomical Society* 441, 3375–3395.
- Xiong, D., Zhang, X., Bai, J., Zhang, H., 2015. Basic properties of fermi blazars and the ‘blazar sequence’. *Monthly Notices of the Royal Astronomical Society* 450, 3568–3578.
- Yan, D., Yang, S., Zhang, P., Dai, B., Wang, J., Zhang, L., 2018. Statistical analysis on xmm-newton x-ray flares of mrk 421: distributions of peak flux and flaring time duration. *The Astrophysical Journal* 864, 164.
- Yang, S., Yan, D., Zhang, P., Dai, B., Zhang, L., 2021. Gaussian process modeling fermi-lat γ -ray blazar variability: A sample of blazars with γ -ray quasi-periodicities. *The Astrophysical Journal* 907, 105.

- Zdziarski, A.A., Mikołajewska, J., Belczyński, K., 2013. Cyg x-3: a low-mass black hole or a neutron star. *Monthly Notices of the Royal Astronomical Society: Letters* 429, L104–L108.
- Zhang, H., Wu, F., Dai, B., 2023a. The detection of possible γ -ray quasi-periodic modulation with 600 days from the blazar s2 0109+ 22. *Publications of the Astronomical Society of the Pacific* 135, 064102.
- Zhang, H., Yan, D., Zhang, L., 2022. Characterizing the γ -ray variability of active galactic nuclei with the stochastic process method. *The Astrophysical Journal* 930, 157.
- Zhang, H., Yan, D., Zhang, L., 2023b. Gaussian process modeling blazar multi-wavelength variability: Indirectly resolving jet structure. *The Astrophysical Journal* 944, 103.
- Zhang, H., Yang, Q., Wu, X.B., 2018. Broadband photometric reverberation mapping analysis on sdss-rm and stripe 82 quasars. *The Astrophysical Journal* 853, 116.
- Zhang, H., Yang, S., Dai, B., 2024a. Discovering the mass-scaled damping timescale from microquasars to blazars. *The Astrophysical Journal Letters* 967, L18.
- Zhang, L., Chen, S., Xiao, H., Cai, J., Fan, J., 2020. Doppler factor estimation for fermi blazars. *The Astrophysical Journal* 897, 10.
- Zhang, X., Xiong, D.r., Gao, Q.g., Yang, G.q., Lu, F.w., Na, W.w., Qin, L.h., 2024b. The fundamental plane of blazars based on the black hole spin-mass energy. *Monthly Notices of the Royal Astronomical Society* 529, 3699–3711.
- Zhou, J., Wang, Z., Chen, L., Wiita, P.J., Vadakkumthani, J., Morrell, N., Zhang, P., Zhang, J., 2018. A 34.5 day quasi-periodic oscillation in γ -ray emission from the blazar pks 2247–131. *Nature communications* 9, 4599.
- Zu, Y., Kochanek, C., Kozłowski, S., Udalski, A., 2013. Is quasar optical variability a damped random walk? *The Astrophysical Journal* 765, 106.

Appendix A. Appendix title 1

Table Appendix A contains information of all sources in our sample.

Source	4FGL name	R.A.	Dec.	Source type	Baseline		z	δ_D	\log (M/M_\odot)	$\ln\tau_{DRW}$ (days)	$\ln\tau_{DRW}$ (days)	$\log_{10}\tau_{\text{year}}$ (days)	Normal Distribution Fitting			Ref.		
					(days)	(days)							μ	σ	KS-test (p-value)			
(1)	(2)	(3)	(4)	(5)	(6)	(7)	(8)	(9)	(10)	(11)	(12)	(13)	(14)	(15)	(16)	(17)	(18)	(19)
S2 0109+22	J0112.1+2245	18.0243	22.7441	BLL	8.81	~5642	0.36	2.59	8.6±0.43	-0.38 ^{+0.15} _{-0.12}	5.26 ^{+0.33} _{-0.26}	2.67 ^{+0.14} _{-0.11}	0.032±0.027	0.26±0.022	1.0	(1)	(2)	(3)
PKS 0735+17	J0738.1+1742	114.531	17.7053	BLL	10.58	~5621	0.424	4.5	8.4±0.42	-0.42 ^{+0.19} _{-0.14}	5.52 ^{+0.40} _{-0.30}	3.39 ^{+0.18} _{-0.13}	0.033±0.019	0.21±0.015	0.98	(4)	(5)	(4)
B2 1215+30	J1217.9+3007	184.467	30.1168	BLL	8.47	~5628	0.113	1.1	8.12±0.41	-0.54 ^{+0.19} _{-0.14}	5.55 ^{+0.42} _{-0.32}	3.54 ^{+0.18} _{-0.15}	0.0422±0.025	0.311±0.020	0.92	(6)	(5)	(7)
B3 1343+451	J1345.5+4453	206.388	44.8832	FSRQ	13.59	~5586	2.534	12.6	8.98±0.99	-0.32 ^{+0.16} _{-0.12}	5.30 ^{+0.34} _{-0.27}	2.85 ^{+0.15} _{-0.12}	-0.0002±0.007	0.09±0.006	0.989	(8)	(9)	(10)
S4 1726+45	J1727.4+4530	261.865	45.511	FSRQ	20.81	~5621	0.717	13.4	8.22±0.411	-0.42 ^{+0.15} _{-0.12}	5.14 ^{+0.37} _{-0.31}	3.11 ^{+0.16} _{-0.13}	-0.006±0.009	0.144±0.007	0.66	(11)	(9)	(12)
S5 1803+78	J1800.6+7828	270.19	78.4678	BLL	8.40	~5642	0.68	5.97	8.6±0.43	-0.04 ^{+0.06} _{-0.06}	3.69 ^{+0.14} _{-0.13}	2.53 ^{+0.10} _{-0.08}	-0.008±0.007	0.033±0.0005	0.167	(13)	(13)	(14)
PKS 2052-47	J2056.2-4714	314.068	-47.2466	FSRQ	11.83	~5481	1.49	17.1	7.88±0.39	-0.29 ^{+0.11} _{-0.09}	4.58 ^{+0.23} _{-0.20}	2.83 ^{+0.10} _{-0.09}	-0.011±0.007	0.10±0.006	0.299	(15)	(15)	(16)
PKS B0027-024	J0030.6-0212	7.6326	-2.1989	BCU	26.78	~3696	1.804	10.3	8.19±0.57	-0.45 ^{+0.15} _{-0.13}	4.55 ^{+0.42} _{-0.36}	2.64 ^{+0.18} _{-0.16}	-0.006±0.020	0.168±0.017	0.786	(17)	(9)	(18)
NGC 1275	J0319.8+4130	49.9507	41.5117	RG	7.20	~5495	0.0176	1.4	7.2±0.44	-0.48 ^{+0.12} _{-0.10}	4.88 ^{+0.26} _{-0.22}	2.25 ^{+0.12} _{-0.09}	0.004±0.003	0.108±0.002	0.98	(20)	(20)	(20)
PMN J0401-2034	J0401.9-2034	60.4696	-20.5861	BCU	27.17	~3479	1.647	13.1	8.19±0.57	-1.26 ^{+0.19} _{-0.18}	4.46 ^{+1.04} _{-0.82}	2.62 ^{+0.45} _{-0.36}	-0.042±0.024	0.215±0.02	0.73	(19)	(9)	(18)
PMN J0948+0022	J0948.9+0022	147.239	0.3737	NLS1	17.11	~5042	0.5846	2.7	7.22±0.32	-0.40 ^{+0.15} _{-0.12}	5.05 ^{+0.38} _{-0.31}	2.50 ^{+0.17} _{-0.13}	-0.025±0.009	0.116±0.007	0.786	(21)	(27)	(21)
Cyg X-3	J2032.6+4053	308.107	40.9577	Microquasar	55.31	~5642	0.003	1.78	0.38±0.26	-0.31 ^{+0.11} _{-0.10}	4.24 ^{+0.29} _{-0.26}	1.83 ^{+0.12} _{-0.11}	0.003±0.005	0.035±0.004	0.351	(22)	(25)	(23)
LS I+61 303	J0240.5+6113	40.1319	61.2293	Microquasar	7.13	~5620	0.0013	1.78	0.6±0.2	-0.28 ^{+0.21} _{-0.15}	5.66 ^{+0.42} _{-0.30}	2.45 ^{+0.18} _{-0.13}	-0.001±0.007	0.263±0.006	0.999	(24)	(25)	(26)

Table A.1: This table provides detailed information on 12 Active Galactic Nuclei (AGNs)—including blazars (BL Lac or FSRQ), radio galaxy (RG), narrow-line Seyfert 1 galaxies (NLS1), and blazar candidates of unclassified type (BCU)—and 2 microquasars. The columns are defined as follows: (1) Source Name, (2) 4FGL Name, (3)-(4) Coordinate of the source, (5) Source Type, (6) Mean cadence (days), (7) Duration of light curve (days) (8) Redshift (z), (9) Doppler Factor (δ_D), (10) Black Hole Mass (in M_\odot unit), (11)-(12) Posterior parameters of modeling the Lightcurves with the DRW process, (13) Damping timescale in the rest frame (days), (14)-(15) Parameters of the Normal distribution fitted to the residuals, (16) Kolmogorov-Smirnov (KS) Test result, (17)-(19)References for the redshift (z), Doppler factor (δ_D), and black hole mass values:(1)Collaboration et al. (2018), (2)Fan et al. (2013), (3)Zhang et al. (2023a)(4)Chai et al. (2012), (5)Liodakis et al. (2017a), (6)Furmiss et al. (2019), (7)Valverde et al. (2020), (8)Sahakyan et al. (2020), (9)Chen (2018), (10)Zhang et al. (2024b), (11)Costamante et al. (2018), (12)Xiong and Zhang (2014), (13)Ghisellini et al. (2010), (14)Lin et al. (2017), (15)Wang et al. (2022), (16)Kadowaki et al. (2015), (17)Peña-Herazo et al. (2021), (18)Xiao et al. (2022), (19)<https://ned.ipac.caltech.edu>, (20)Zhang et al. (2022), (21)Xin et al. (2022), (22)Koljonen and Tomsick (2020), (23)Zdziarski et al. (2013), (24)<https://simbad.u-strasbg.fr/simbad/sim-fbasic>, (25)Molina et al. (2019), (26)Massi et al. (2017), (27)Doi et al. (2019)